PHYSICAL REVIEW E **72**, 060701(R) (2005)

Paraelectric-antiferroelectric phase transition in achiral liquid crystals

Damian Pociecha,[1] Ewa Gorecka,[1] Mojca Čepič,[2] Nataša Vaupotič,[2,3] Kinga Gomola,[1] and Jozef Mieczkowski[1,4]
[1]*Department of Chemistry, Warsaw University, Al. Zwirki i Wigury 101, 02-089 Warsaw, Poland*
[2]*Jozef Stefan Institute, Jamova 39, 1000 Ljubljana, Slovenia*
[3]*Faculty of Education, Koroška 160, 2000 Maribor, Slovenia*
[4]*Institute of Chemistry, Military University of Technology, 00-908 Warsaw, Poland*
(Received 23 June 2005; published 21 December 2005)

Critical freezing of molecular rotation in an achiral smectic phase, which leads to polar ordering through the second order paraelectric-antiferroelectric (Sm-$A \rightarrow$ Sm-AP_A) phase transition is studied theoretically and experimentally. Strong softening of the polar mode in the Sm-A phase and highly intensive dielectric mode in the Sm-AP_A phase are observed due to weak antiferroelectric interactions in the system. In the Sm-AP_A phase the dielectric response behaves critically upon biasing by a dc electric field. Such a behavior is found general for the antiferroelectric smectic phase with significant quadrupolar interlayer coupling.

DOI: 10.1103/PhysRevE.72.060701 PACS number(s): 61.30.Cz, 64.70.Md, 77.22.Gm, 77.84.Nh

The nature of the transition from the paraelectric to the polarly ordered phase was studied extensively for a number of solid crystals [1] as well as for chiral liquid crystals (LC) [2,3]. In crystals the transition to the ferroelectric or the antiferroelectric state is associated with a condensation of fluctuations related to the lattice motion. In chiral LCs the spontaneous electric polarization is a consequence of the tilt of the molecules with respect to the layer normal. Basic excitations of polarization are thus coupled to the fluctuations in the magnitude of the tilt (amplitude fluctuations) or the direction of the tilt (phase fluctuations). On the other hand, only little is known about the development of polar order in the achiral LC systems. The achiral LCs, made of bent-shaped molecules, represent a class of mesogenic materials [4] in which the polar order can appear independent of the molecular tilt. The polar order in such materials results from steric interactions among the strongly bent molecules. These hinder the molecular rotation which leads to the ordering of the dipole moments.

In this paper a model system is studied in which polar order develops due to the collective freezing of the molecular rotation. A homolog series of achiral materials is investigated, which, upon reduction of temperature, exhibit a continuous phase transition from the paraelectric smectic-A (Sm-A) phase to the polar, nontilted antiferroelectric Sm-AP_A phase. Materials with such polymorphism are rare [5,6] since the vast majority of the bent-core mesogens tend to form polar, tilted phases [7]. The system exhibits critical slowing down of polar fluctuations in the paraelectric Sm-A phase upon approaching the phase transition temperature to the antiferroelectric Sm-AP_A phase. An exceptionally strong dielectric mode observed in the Sm-AP_A phase shows that the antiferroelectric coupling of the layer polarization in the Sm-AP_A phase is weak. The dielectric response in the Sm-AP_A phase is also strongly sensitive to the bias electric field. Close to the threshold field from the antiferroelectric to the induced ferroelectric state the dielectric response increases as the polarization phase fluctuations critically slow down. We show that such a behavior is general for the antiferroelectric smectic phase with significant quadrupolar interlayer coupling.

The system is described theoretically by a discrete phenomenological model. Despite the fact that the Sm-AP_A phase is an improper polar phase [1–3], in which the polar order is a consequence of the restricted molecular rotation, the order parameter appropriate for the second order Sm-$A \rightarrow$ Sm-AP_A transition is the polarization vector $\mathbf{P}_j$, which is the space averaged transverse dipole moment in the jth smectic layer [Fig. 1(a)]. The free energy (G) of the system is given as

$$G = \sum_j \frac{1}{4}a_0(\mathbf{P}_j^2 + \mathbf{P}_{j+1}^2) + \frac{1}{8}b_0(\mathbf{P}_j^4 + \mathbf{P}_{j+1}^4) + \frac{1}{2}a_1(\mathbf{P}_j \cdot \mathbf{P}_{j+1}) - \frac{1}{4}b_Q(\mathbf{P}_j \cdot \mathbf{P}_{j+1})^2 - \frac{1}{2}\mathbf{E} \cdot (\mathbf{P}_j + \mathbf{P}_{j+1}). \quad (1)$$

The parameter $a_0 = a(T - T_0)$ changes sign at temperature T_0, the parameter b_0 is positive. For the positive coupling constant a_1 the antiferroelectric ordering in the neighboring layers is favored below the phase transition temperature from the Sm-A to the Sm-AP_A phase given by $T_P = T_0 + a_1/a$. The positive parameter b_Q describes the quadrupolar coupling that favors parallel or antiparallel ordering of dipoles in the neighboring layers. **E** is the external electric field. Assuming

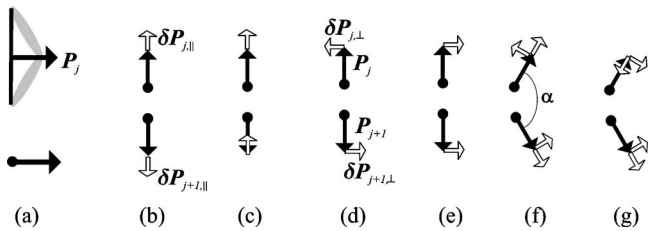

FIG. 1. (a) Definition of P_j (see text). Collective fluctuations in the Sm-AP_A phase: in-phase (b) and antiphase (c) amplitudons, in-phase (d) and antiphase (e) phasons. In dielectric measurements only antiphase modes are active. The dc bias field distorts the structure ($\alpha < \pi$), therefore both in-phase (f) and antiphase (g) modes become polar and dielectrically active.

that $P_j = P_{j+1} = P_0$ is the magnitude of the equilibrium polarization in zero external field at

$$T < T_P,\ P_0 = \sqrt{a(T_P - T)/(b_0 - b_Q)}.$$

In the Sm-*A* phase, there is no net polarization, but thermally excited collective fluctuations lead to the appearance of a local polarization $\boldsymbol{\delta P}_j$. Fluctuations can be detected by the coupling of the induced polarization $\boldsymbol{\delta P}_j$ to the electric field. In the dielectric spectroscopy polarization wave with the wave vector $q=0$ ($\boldsymbol{\delta P}_j = \boldsymbol{\delta P}_0$ for all layers) is measured. Applying the Landau-Khalatnikov relaxation equation to the free energy density expanded up to the second order terms in $\boldsymbol{\delta P}_0$ the mode relaxation frequency ω_0 is found. It lowers linearly with temperature as $\omega_0 = [a(T - T_P) + 2a_1]/\gamma$, where γ is the viscosity. This indicates softening of the ferroelectric fluctuations in the paraelectric Sm-*A* phase close to the transition to the antiferroelectric Sm-AP_A phase.

In the Sm-AP_A phase the instantaneous polarization is given by $\mathbf{P}_j = \mathbf{P}_{j0} + \boldsymbol{\delta P}_{j\parallel} + \boldsymbol{\delta P}_{j\perp}$, where $\boldsymbol{\delta P}_{j\parallel}, \boldsymbol{\delta P}_{j\perp}$ are fluctuations of polarization parallel and perpendicular to the direction of the polarization $\mathbf{P}_{j0}$, respectively. The same procedure as used in the Sm-*A* phase leads to two elementary excitations active in the homogenous ac electric field, with eigenfrequencies,

$$\omega_{\parallel 0} = \frac{2}{\gamma}\left[a(T_P - T) + 2a\frac{b_Q}{b_0 - b_Q}(T_P - T) + a_1 \right],$$

$$\omega_{\perp 0} = \frac{2}{\gamma}\left[a\frac{b_Q}{b_0}(T_P - T) + a_1 \right].$$

The first mode is the antiphase amplitudon [3] [Fig. 1(c)]. Its frequency lowers near the phase transition temperature to a finite value at the transition. The second mode is the antiphase phason [Fig. 1(e)] and it is almost temperature independent if $b_Q \ll b_0$.

The dielectric response in the Sm-AP_A phase becomes more complex if the system is biased by an external dc electric field E_B. If the field is applied in the direction perpendicular to the undistorted polarization, the antiferroelectric structure becomes distorted as shown in Figs. 1(f) and 1(g) and additional modes become active [8]. Since the angle α between the polarizations in the neighboring layers reduces from π, the antiphase phason fluctuations are enhanced. The antiphase phason relaxation frequency depends on the bias electric field in a complex way:

$$\omega_\perp(E_B) = \omega_{\perp 0} - (a_1/\gamma)\cos^2(\alpha/2) - (3b_Q/2\gamma)P_0^2 \sin^2(\alpha),$$

where $\omega_{\perp 0}$ is the relaxation frequency in the nondistorted antiferroelectric structure and P_0 and α both depend on E_B. The maximum dielectric strength of the antiphase phason is given by $\Delta\varepsilon_\perp = A/\omega_\perp$, where A depends on E_B and α as well. A and $\omega_\perp$ can be calculated only numerically and their dependence on E_B is shown in Fig. 6. Neglecting the quadrupolar coupling ($b_Q = 0$) makes this dielectric response almost independent of E_B since both A and $\omega_\perp$ decrease equally with an increasing bias field (Fig. 6). Including the quadrupolar coupling, there are two minima in the free energy—one corresponding to the antiferroelectric structure and one to the ferroelectric structure, thus the first order transition to ferroelectric state is allowed [9,10] at the threshold value of the bias field (E_{th}). Close to the threshold field the dielectric response increases significantly due to the more rapid decrease of $\omega_\perp$ (almost to zero at E_{th}) than of the parameter A. Weak dependence of parameter A on E_B is caused by only a small deviation of angle α, which even at E_{th} remains far from zero. Above the threshold field, in the induced ferroelectric phase, the phason is suddenly quenched and only the amplitudon, which has two orders of magnitude higher frequency and thus lower dielectric response, remains active.

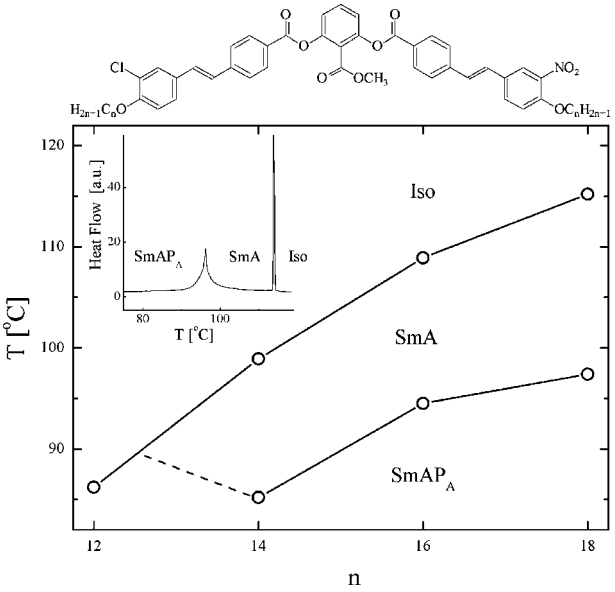

FIG. 2. A general chemical formula and a phase diagram for the studied homolog series, *n* denotes the length of the terminal alkyl chains. Inset: DSC scan showing noticeable heat capacity anomalies at both sides of the Sm-$A \rightarrow$ Sm-AP_A phase transition.

Experimentally, the Sm-$A \rightarrow$ Sm-AP_A phase sequence was found in three newly obtained compounds belonging to the homolog series of asymmetric bent shaped molecules (Fig. 2). The phase transition temperatures were determined by DSC (Perkin Elmer DSC 7) and optical methods (polarizing microscope Nikon Optiphot2-Pol). The Sm-*A* phase temperature range increases with elongation of terminal alkyl chains (Fig. 2), indicating that the rotation freedom of molecules increases as the mesogenic core to terminal chain length ratio decreases. In DSC scans at the Sm-*A*-Sm-AP_A phase transition pronounced heat capacity anomalies are visible in both phases (inset in Fig. 2). In the homeotropically aligned samples the Sm-*A* phase exhibits uniform dark texture pointing to optical uniaxiality of the phase, while the transition to the Sm-AP_A phase is observed as an appearance of schlieren texture, with $s = \pm 1$ defects. The brightness of the schlieren texture gradually increases as birefringence continuously increases from zero in the Sm-*A* phase. Continuous increase of birefringence is characteristic of the second order phase transition. X-ray studies (DRON diffractometer working in reflection mode) have shown that the layer spacing increases continuously through the Sm-$A \rightarrow$ Sm-AP_A phase transition (Fig. 3). The increase, although continuous for all materials, is more pronounced and abrupt for longer homologs. Ob-

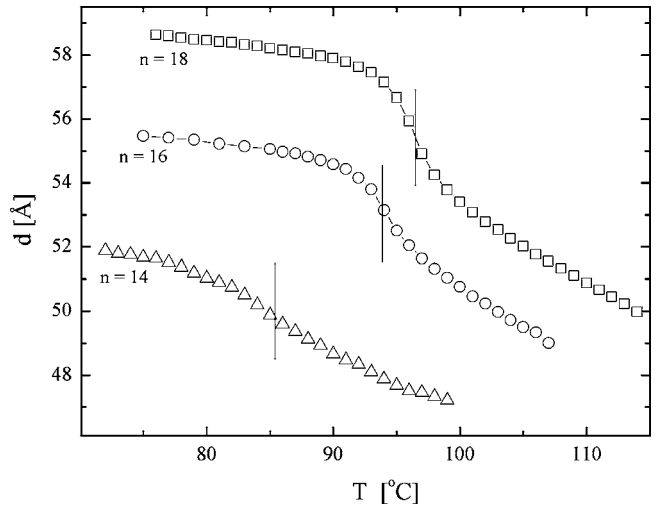

FIG. 3. Layer spacing vs temperature in the vicinity of the Sm-A-Sm-AP_A phase transition.

served changes in the layer spacing might result from an increasing orientational order parameter, which is apparently coupled to the polar order. The molecular conformation change from the rodlike (longer molecular length) to the bent-core (shorter molecular length) shape, observed previously [11], thus cannot be the driving mechanism for the transition from the paralectric to the polar phase in the present materials.

The switching of electric polarization upon reversal of the applied electric field is observed in a low temperature phase and the double current peak unambiguously confirms the antiferoelectric nature of the Sm-AP_A phase (inset in Fig. 4). The value of electric polarization, which for all homologs, far from the transition point is $\sim$300 nC cm^{-2}, is typical for

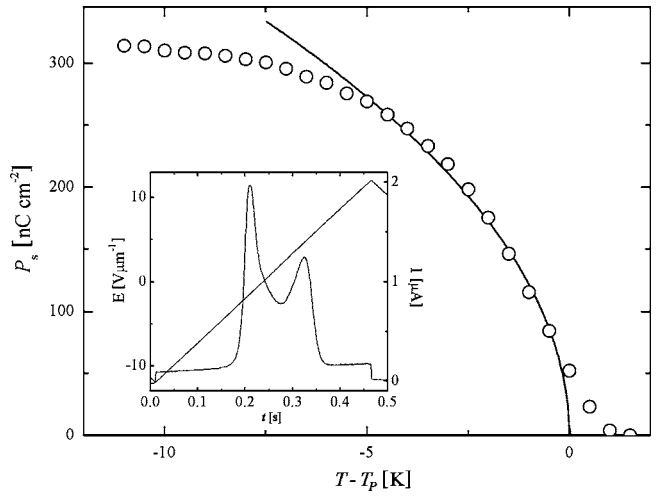

FIG. 4. Spontaneous polarization vs temperature for the compound with $n=18$. The fit to the power low with critical exponent 0.5 is given as a guide for the eye. Far from the transition the polarization becomes saturated. The inset: the current response in the Sm-AP_A phase at $T=90$ °C. The nonequal amplitudes of both current peaks indicate that the one at $E\sim 0$ apart from the ferro-antiferro state change also has a significant contribution resulting from the direct ferro-ferro state change.

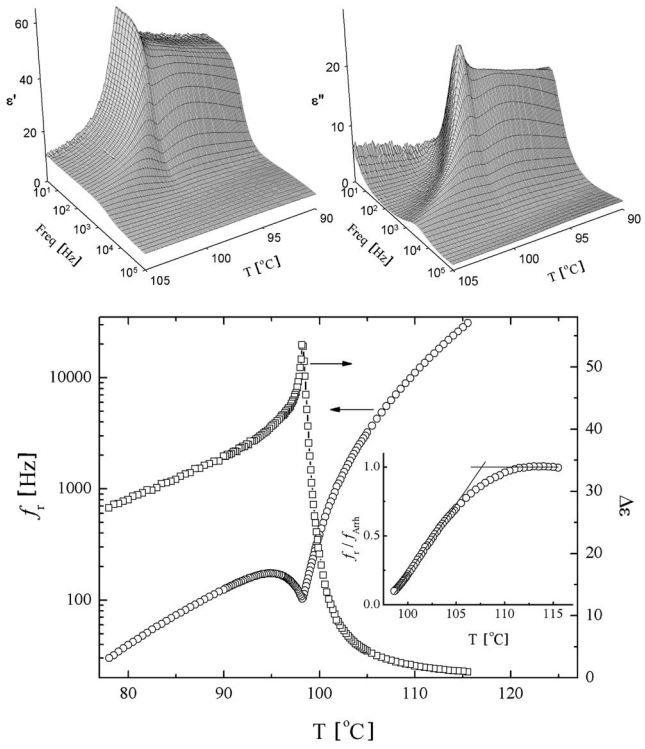

FIG. 5. Three-dimensional (3D) temperature-frequency plot of the real and imaginary parts of the dielectric constant for compound $n=18$. Two-dimensional (2D) graph: the relaxation frequency f_r and the dielectric strength $\Delta\varepsilon$ of the mode vs temperature obtained by fitting the Cole-Cole formula. The inset: critical part of the relaxation frequency calculated as f_r/f_{rArrh} (f_{rArrh} was determined from data taken above 111 °C and extrapolated to lower temperatures) showing linear decrease on approaching the phase transition.

bent-core mesogens. It continuously falls down to zero on approaching the paraelectric phase (Fig. 4), however a critical exponent cannot be determined precisely due to the strong nonlinear dielectric susceptibility of the system near the phase transition that contributes to the current response and obscures the polarization measurements. The switching of polarization occurs without changes of optical extinction directions, as expected for a nontilted phase. The dielectric dispersion measurements (Fig. 5) performed in a broad temperature range (Solartron SI 1260 Impedance Analyzer, 1–10^7 Hz frequency range, ITO cells with planar alignment, 3–5 μm-thick) show a nearly monodispersive relaxation process, the parameter in the Cole-Cole formula, which is a measure of the width of relaxation frequency distribution, is below 0.05, except for the close vicinity of the phase transition where it increases to 0.1. In the Sm-A phase, far from the phase transition the relaxation frequency follows the Arrhenius law: $f_{Arrh}=f_0 e^{-E_a/kT}$, with $E_a=220$ kJ mol^{-1} and 300 kJ mol^{-1} for materials with $n=18$ and $n=16$, respectively. On approaching the Sm-$A\rightarrow$Sm-AP_A phase transition temperature the molecular motions become collective and the dielectric response shows crossover behavior, in which f_0 becomes temperature dependent: $f_0=A(T-T_P)+f_0^c$ (inset Fig. 5). For all homologs the relaxation frequency f_0^c at the phase transition temperature is $\sim$100 Hz, which indicates that the

ferroelectric mode is nearly condensed. The frequency f_0^c is proportional to the parameter a_1 in the theoretical model. Its small value shows that antiferroelectric interactions are weak in the studied system. For comparison, in rodlike material showing the Sm-$A \rightarrow$ Sm-C_A^* phase sequence the antiferroelectric interlayer interactions are much stronger, as indicated by f_0^c, which is three orders of magnitude higher [12]. The critical dependence of the relaxation frequency is also visible below T_P. This is due to the temperature dependence of the antiphase amplitudon mode active in the Sm-AP_A phase. However, far from the transition, the main contribution to the dielectric response comes from antiphase phason. Due to the weak interlayer coupling the antiphase phason in the Sm-AP_A phase is considerably stronger, $\Delta\varepsilon \sim 30$, and of lower relaxation frequency than in antiferroelectric rodlike systems, where $\Delta\varepsilon \sim 1$ [13]. Application of a dc bias electric field to the sample has a profound effect on the dielectric response in the Sm-AP_A phase (Fig. 6). With an increase of the bias electric field, the dielectric strength of the mode increases gradually and shows maximum at the critical field E_{th}, which is the field that switches the polarizations in the neighboring layers from antiparallel to parallel arrangement. The anomal increase of the dielectric mode strength on approaching E_{th} is accompanied by a slowing down of the related relaxation process. Such a behavior of the mode is in agreement with theoretical predictions for the antiphase phason, where the proper shape of f_r and $\Delta\varepsilon$ dependence on E_B is obtained (Fig. 6) for the ratio of parameters describing antiferropolar to quadrupolar interlayer coupling $a_1 P_0^2/(b_Q P_0^4) \approx 2.5$. In the induced ferroelectric phase, above E_{th}, only an amplitudon mode is observed that is strongly quenched due to the saturation of P against E. Although application of the bias electric field could also excite the in-phase modes (phason and amplitudon), their contribution to the dielectric response should be negligible in the studied sample geometry, with the measuring ac field along the bias dc field. This is also confirmed by numerical calculations.

To summarize, the presented system shows the transition from the noncollective to the collective molecular motions, which manifests itself in the critical slowing down of the motion dynamics as the Sm-A phase approaches the polar instability. Due to a much weaker interlayer antiferroelectric interactions the softening of the polar mode is much stronger than observed at the Sm-$A \rightarrow$ Sm-C_A^* phase transition in the chiral tilted smectics. The weak antiferroelectric coupling is also responsible for an exceptionally strong antiphase phason mode in the Sm-AP_A phase; its dielectric strength is of the order of magnitude higher and relaxation frequency of three orders of magnitude lower than usually found for chiral antiferroelectric Sm-C_A^* phase. Moreover, the phason in the Sm-AP_A behaves critically when biased by a dc electric field, its strength is maximal and the frequency is minimal at the threshold field that induces the ferroelectric state. Above the threshold field the mode is suddenly quenched. This can be explained by quadrupolar interlayer coupling that prevents strong distortion of dipoles from an antiferroelectric arrangement and allows the first order transition to the ferroelectric state.

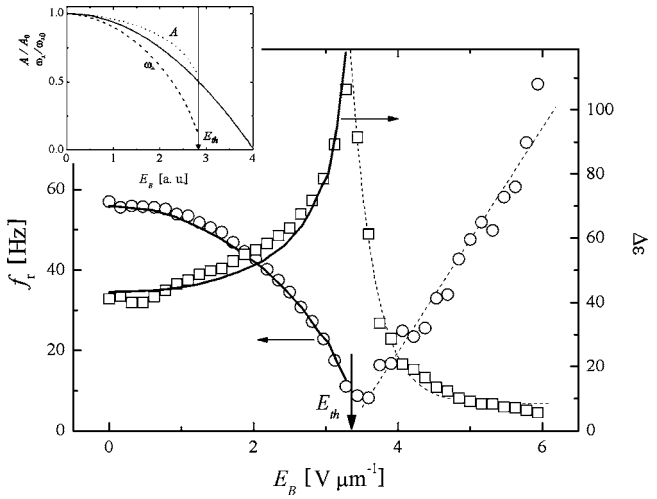

FIG. 6. Relaxation frequency f_r and the dielectric strength $\Delta\varepsilon$ of the mode vs bias dc field for material $n=18$ in the Sm-AP_A phase at 86 °C. The solid lines below the threshold field E_{th} are obtained from the model describing behavior of the antiphase phason under the bias field. Dashed lines above E_{th} are guides for the eye. Inset: Dependence of A and $\omega_\perp$ on E_B at finite b_Q (dashed and dotted line) and at $b_Q=0$ (solid line) where both curves coincide. A_0 and $\omega_{0\perp}$ are the values at zero bias field.

This work was supported by the KBN grant 4T09A 00425 and the Polish-Slovenian Cooperation Joint Project.

[1] M. E. Line and M. Glass, *Principle and Aplications of Ferrolectric and Related Materials* (Oxford University Press, Oxford, 2001).
[2] S. T. Lagerwall, *Ferroelectric and Antiferroelectric Liquid Crystals* (Wiley, New York, 1999).
[3] I. Muševič, R. Blinc, and B. Žekš, *The Physics of Ferroelectric and Antiferroelectric Liquid Crystals* (World Scientific, Singapore, 2000).
[4] T. Niori *et al.*, J. Mater. Chem. **6**, 1231 (1996).
[5] A. Eremin *et al.*, Phys. Chem. Chem. Phys. **6**, 1290 (2004).
[6] R. A. Reddy and B. K. Sadashiva, J. Mater. Chem. **14**, 310 (2004).
[7] D. R. Link *et al.*, Nature **278**, 1924 (1998).
[8] L. A. Parry-Jones and S. J. Elston, J. Appl. Phys. **92**, 449 (2002).
[9] D. Pociecha *et al.*, Phys. Rev. Lett. **86**, 3048 (2001).
[10] L. A. Parry-Jones and S. J. Elston, Appl. Phys. Lett. **79**, 2097 (2001).
[11] I. Wirth *et al.*, J. Mater. Chem. **11**, 1642 (2001).
[12] K. Hiraoka *et al.*, Mol. Cryst. Liq. Cryst. **199**, 197 (1991).
[13] S. Merino *et al.*, Phys. Rev. E **54**, 5169 (1996).